Determination of Partition Coefficient of Spin Probe between Different Lipid Membrane Phases

Zoran Arsov* and Janez Štrancar

Laboratory of Biophysics, "Jožef Stefan" Institute, Jamova 39, 1000 Ljubljana, Slovenia

Received May 1, 2005

Model lipid membranes made from binary mixtures of dimyristoylphosphatidylcholine/dipalmitoylphosphatidylcholine (DMPC/DPPC) and dimyristoylphosphatidylcholine/cholesterol (DMPC/Chol) exhibit coexistence of diverse lipid phases at appropriate temperature and composition. Since lipids in different phases show different structural and motional properties, it is expected that the corresponding spin probe electron paramagnetic resonance (EPR) spectra will be superposition of several spectral components. From comparison of proportions of spectral components of the EPR spectrum with the fractions of the corresponding lipid phases obtained from known phase diagrams the partition coefficient of spin probe methyl ester of 5-doxyl palmitate between different lipid phases was determined. The results indicate that the used spin probe partitions approximately equally between different phases.

INTRODUCTION

Model membranes composed of different lipid constituents exhibit lateral phase separation at appropriate temperature and composition.[1] Since structural and motional properties of lipids vary between different phases, it is expected that for slow exchange between different membrane compartments the corresponding spin probe electron paramagnetic resonance (EPR) spectra will be superposition of several spectral components. Also biological membranes have heterogeneous structures exhibiting coexistence of different lateral lipid domains. A lateral lipid domain is considered to be a spatially limited region of membrane distinguished from its neighboring regions by one or more measurable properties;[2] a group of domains with similar properties represents a particular domain type. Consequently, similar to model membranes also in biological membranes one can expect that the EPR spectra will be composed of different spectral components.

Within the procedure of the EPR spectra decomposition also proportions of particular spectral components can be determined from their relative intensities,[3] which can give an estimate of the fraction of a particular lipid phase (domain type) in the lipid membrane. However, one has to be aware that the proportion of a particular spectral component is not necessarily the same as the fraction of the corresponding lipid phase (domain type) in the membrane, as the determined proportions have to be corrected according to partitioning properties of spin probe between different lipid phases (domain types). This problem is schematically presented in Figure 1. From the comparison of the measured temperature dependence of the proportions of spectral components of the EPR spectra and the calculated temperature dependence of fractions of corresponding lipid phases the partition coefficient of spin probe can be determined. Such a procedure in the case of fluorescence probes was already described by Mesquita et al.[4]

* Corresponding author phone: +386 1 477 36 48; fax: +386 1 477 31 91; e-mail: zoran.arsov@ijs.si.

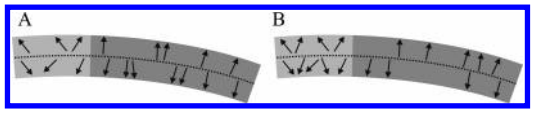

Figure 1. Schematic presentation of the effect of a partition coefficient of a spin probe between different lipid phases on relation between the lipid phase fractions and proportions of corresponding spectral components. The lipid bilayer is composed of two lipid phases, a light gray patch and a dark gray patch, respectively. Spin probe molecules are denoted by arrows. Fractions of lipid phases are determined from a number of lipid molecules in a particular phase relative to their total number; schematically they correspond to the size of the patches in the figure. The proportions of corresponding spectral components are determined from their relative intensities, that is from a number of spin probe molecules in a particular phase relative to their total number; schematically they correspond to the number of arrows in a particular patch. (A) An example of equal partitioning between phases, where we expect that the fractions of lipid phases will be similar to the proportions of corresponding spectral components. (B) An example of higher partitioning of the spin probe in the light gray patch of the bilayer, where we expect that the proportion of a spectral component corresponding to the light gray patch will increase (on account of the proportion of the dark gray patch) and consequently will be higher than the fraction of the light gray patch.

It is important to know the partitioning properties of spin probes when accurate estimates for fractions of lipid domain types have to be obtained, for example when using a lipid domain approach to describe the activity of membrane-bound enzymes.[5] Since the enzyme activity may change between different domain types, the overall activity A can be calculated as a weighted sum of the local enzyme activities A_i in a particular domain type i

$$A = \sum_i f^i A_i \qquad (1)$$

where f^i is the fraction of lipid domain type i. To determine A_i the properties of each domain type should be characterized, while for estimating the contribution of a particular domain type to the overall expression of property A also fractions f^i have to be determined. In general A may represent any membrane-dependent property.

10.1021/ci0501793 CCC: $30.25
Published on Web 10/20/2005

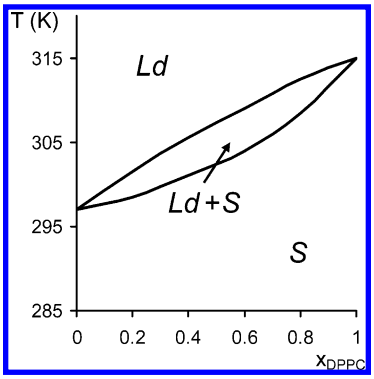

Figure 2. Temperature-composition phase diagram for lipid mixture DMPC/DPPC with marked lipid phases and lipid phase coexistence regions (adapted from Mabrey and Sturtevant):[6] gel phase *S*, liquid-disordered phase *Ld*, and coexistence region of phases *Ld* and *S* (*Ld*+*S*). The DPPC mole fraction is denoted by x_{DPPC}. Lines represent phase boundaries between different phase regions.

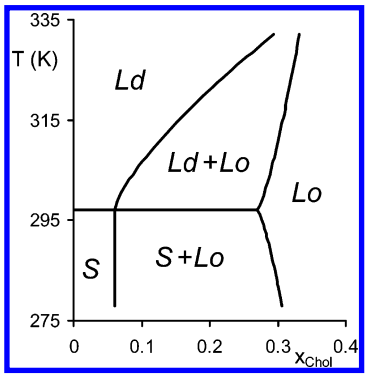

Figure 3. Temperature-composition phase diagram for the lipid mixture DMPC/Chol with marked lipid phases and lipid phase coexistence regions (adapted from Almeida et al.):[7] gel phase *S*, liquid-ordered phase *Lo*, liquid-disordered phase *Ld*, and coexistence regions of phases *S* and *Lo* (*S*+*Lo*) and of phases *Ld* and *Lo* (*Ld*+*Lo*). The cholesterol mole fraction is denoted by x_{Chol}. Lines represent phase boundaries between different phase regions. At the horizontal line (temperature T_m) the main phase transition occurs.

In our experiments two binary lipid mixtures showing lateral phase separation were examined: dimyristoylphosphatidylcholine/dipalmitoylphosphatidylcholine (DMPC/DPPC) and dimyristoylphosphatidylcholine/cholesterol (DMPC/Chol). In the first mixture two different lipid phases can be present, gel phase *S* and liquid-disordered phase *Ld*, respectively, whereas in the second mixture also liquid-ordered phase *Lo* can be present besides phases *S* and *Ld*. In the studied temperature interval the first mixture exhibits the coexistence of liquid-disordered phase and gel phase *Ld*+*S* (Figure 2), while the second mixture exhibits two coexistence regions, one composed of gel phase and liquid-ordered phase *S*+*Lo* and the other composed of liquid-disordered phase and liquid-ordered phase *Ld*+*Lo* (Figure 3).

As there are many indications that lateral lipid domains, the so-called lipid rafts, with properties similar to the *Lo* phase are present in biological membranes,[8−10] the mixture DMPC/Chol is especially interesting, due to the *Ld*/*Lo* phase separation at the appropriate temperature and amount of cholesterol. Determination of the partition coefficient between the two lipid phases, *Ld* and *Lo* phases, respectively, could therefore enable a more accurate estimate of fractions of lipid domain types in lipid bilayers of lipid mixtures, whose phase diagrams are not known. Furthermore, it could enable a valuable characterization of coexistence of different domain types in terms of their fractions even for biological membranes.

From known phase diagrams fractions of particular lipid phases can be determined at certain temperatures and composition. In addition, EPR spectra decomposition enables determination of proportions of corresponding spectral components and by that EPR-estimated fractions of lipid phases. Since phase diagrams for binary mixtures DMPC/DPPC and DMPC/Chol show coexistence of two lipid phases, EPR spectra were decomposed into two spectral components. From comparison of proportions of spectral components of the EPR spectrum and the fractions of corresponding lipid phases the partition coefficient of spin probe MeFASL(10,3) (methyl ester of 5-doxyl palmitate) between different lipid phases in the observed lipid mixtures was established.

MATERIALS AND METHODS

Preparation of Liposomes. Two sorts of liposomes with varying relative compositions were made: DMPC/DPPC and DMPC/Chol. Each time 50 mg of the appropriate mixture of dry lipids (obtained from Avanti Polar Lipids, Birmingham, AL, and cholesterol Sigma) was dissolved in 1.4 mL of chloroform and 0.7 mL of methanol. The organic solvents were evaporated on a rotary evaporator and a vacuum pump in a glass flask forming a lipid film. One milliliter of phosphate buffer saline (PBS; 290 mOsmol/kg, pH 7.4) was added to the flask. The suspension was hand-shaken and then left to hydrate for approximately 45 min at a temperature 10 degrees above the main phase transition of the corresponding lipid mixture.

Spin Labeling and EPR Spectra Acquisition. One hundred microliters of 10^{-4} M solution in ethanol of a lipophilic spin probe, methyl ester of 5-doxyl palmitate MeFASL(10,3) (nitroxide radical as spin label), was added to the plastic tube. A thin film of spin probes deposited on the walls of the glass tube was formed by evaporation of ethanol. One hundred microliters of prepared liposomes was added to the tube. The tube was then rotated for 5 min at a temperature 10 degrees above the main phase transition of the corresponding lipid mixture and subsequently hand-shaken for 3 min. The labeled sample was transferred into a quartz-glass capillary of 1-mm inner diameter, and the EPR spectrum was recorded on a Bruker ESP 300E spectrometer (Karlsruhe, Germany) with a microwave frequency of 9.59 GHz and power of 20 mW, a modulation frequency of 100 kHz, and an amplitude of 0.05 mT. The ratio of the number of spin probe molecules to the number of lipid molecules was approximately 1/700.

EPR Spectra Decomposition and Determination of Proportions of Spectral Components. The recorded EPR spectra were characterized using spectrum simulation. Generally, to describe the EPR spectra of spin labels, the stochastic Liouville equation is used.[11] However, in a membrane system labeled with fatty acid spin probes measured at physiological temperatures, the majority of the local rotational motions is fast with respect to the EPR time scale. Since the fast motion approximation is around 100 times less computationally demanding, it is therefore reasonable to simplify the modeling of the spectra taken at

physiological temperatures by restricting the motions to the fast motional regime. In addition, molecular dynamics simulations show that conformational motions are much faster than the EPR time scale even for lower temperatures.[12,13] Consequently, the spectrum-simulation model was the so-called motional-restricted fast-motion approximation.[14]

In a membrane system, where conformational rotational motions are fast with respect to the EPR time scale, the magnetic interaction tensors can be averaged over the stochastic rotational motions of spin probes. The effect of slower molecular motions at low temperatures is neglected to maintain a numerically well-posed model. Subsequently, the spin Hamiltonian with averaged tensor components can be used to calculate line positions for the spin-probe molecules in membrane segments with their particular orientation relative to the external magnetic field. The spectra of the randomly oriented cell membrane segments are finally summed to get the inhomogeneously broadened stick spectra, which is further convoluted with a Lorentzian line shape to get the final line shape of the simulated EPR spectrum. The spectral parameter set consists of order parameter, effective rotational correlation time, additional broadening constant, and hyperfine and Zeeman tensors' polarity correction factors. The software EPRSIM[15] allows us to decompose a spectrum $I(B)$ into a different number of spectral components $I_i(B)$ related to the lipid phases (domain types)

$$I(B) = \sum_i w^i I_i(B) \tag{2}$$

where w^i is the proportion of the spectral component i and B is the magnetic field.

The parameters of the model were searched by a hybrid-evolutionary-optimization (HEO) procedure, which combines the deterministic simplex algorithm and the stochastic genetic algorithm.[16,17] HEO belongs to the class of the stochastic and population based optimization algorithms. Since it is not sensitive to a starting population, this can be generated randomly eliminating human input and thus enabling an automatic optimization. Before the optimization is started the number of spectral components is chosen. To guide the optimization reduced χ^2 was introduced as a fitness function, which measures the goodness of fit of the simulated spectrum to the experimental one. The errors of spectral parameters are calculated from diagonal elements of the covariance matrix and the correlation coefficients from the off-diagonal elements. At the same time the stochastic nature of HEO optimization allows us to determine the errors in the spectral parameters independently of the covariance matrix analysis.

Each spectrum was optimized only six times representing a balance between statistical requirements and minimization of computational time. It is also worth remembering that the probability of finding the real global minimum in a single run is very high due to the use of the stochastic genetic algorithm. Besides comparison of χ^2 values the best fit was also assessed visually from a set of fits provided by multiple runs of the optimization. The parameters of the best fit were used to present the results.

Calculation of Proportion of Spectral Component from Fraction of Lipid Phase and Partition Coefficient of Spin Probe. In a binary lipid mixture of lipid 1 and lipid 2 regions of at most two lipid phases can coexist according to the Gibbs' phase rule. Let us denote the two phases by indices u and v. Regions of single and coexisting lipid phases in a lipid phase diagram are divided by phase boundaries, which can be given in terms of mole fractions x of lipid 2

$$x_2^i = N_2^i/(N_1^i + N_2^i) = N_2^i/N^i \tag{3}$$

where $N_1{}^i$ and $N_2{}^i$ represent the number of lipid molecules 1 and 2, respectively, in phase i ($i = u, v$) with their sum denoted as $N^i = N_1{}^i + N_2{}^i$. The total number of lipids will be denoted N.

In experiment the mole fraction $x_2{}^0$ of lipid 2 is varied. At a certain $x_2{}^0$ the fraction of lipids $f^u = N^u/N$ in phase u at temperature T can be expressed with mole fractions of lipid 2 at phase boundaries $x_2{}^u$ and $x_2{}^v$ (eq 3) through the so-called lever rule:

$$f^u(T) = \frac{x_2^v(T) - x_2^0}{x_2^v(T) - x_2^u(T)} \tag{4}$$

The corresponding types of lipids and lipid phases for each lipid mixture are summarized in Table 1 (see also phase diagrams in Figures 2 and 3 for reference). Temperature T_m in Table 1 represents the temperature of the main phase transition in the case of DMPC/Chol mixture (see Figure 3).

Table 1. Types of Lipids and Lipid Phases in Our Experiments

mixture	lipid 1	lipid 2	lipid phase u	lipid phase v
DMPC/DPPC	DMPC	DPPC	*Ld*	*S*
DMPC/Chol ($T < T_m$)	DMPC	Chol	*S*	*Lo*
DMPC/Chol ($T > T_m$)	DMPC	Chol	*Ld*	*Lo*

The calculated fraction of lipids in each phase will be compared to the proportions of the spectral components of an EPR spectrum, corresponding to a particular lipid phase, enabling extraction of the partition coefficient K of spin probe between different lipid phases. At this point we have to emphasize that we will not take into account partitioning of spin probes in the buffer phase of the system, while the used spin probe is strongly lipophilic. It is therefore reasonable to expect that only a very small amount of spin probe molecules will not be inserted into the lipid membrane and that the effect of water phase on partitioning can be neglected.

The partition coefficient for spin probe can be derived from the equilibrium condition for chemical potentials. The chemical potential (expressed with regard to the number of molecules) of spin probe s in a particular lipid phase i ($i = u, v$) can be written as

$$\mu_s^i = \mu_{s,0}^i + kT \ln x_s^i \tag{5}$$

where $\mu_{s,0}{}^i$ is the standard chemical potential of the pure phase i, k is the Boltzman constant, and x_s^i is the mole fraction of the spin probe in phase i. In equilibrium we have $\mu_s^u = \mu_s^v$, so that from eq 5 we can define partition coefficient K^x as

$$\ln\frac{x_s^u}{x_s^v} = \ln K^x = \frac{1}{kT}(\mu_{s,0}^v - \mu_{s,0}^u) \tag{6}$$

With the number of spin probe molecules N_s^u and N_s^v in lipid phases u and v, respectively, and the total number of spin probes denoted as N_s the partition coefficient can be expressed as

$$K^x = \frac{x_s^u}{x_s^v} = \frac{N_s^u/(N_s^u + N^u)}{N_s^v/(N_s^v + N^v)} \approx \frac{N_s^u}{N_s^v}\frac{N^v}{N^u} \tag{7}$$

where the expression was simplified for small concentrations of spin probe. Taking into account that the proportion of the spectral component corresponding to the lipid phase u is $w^u = N_s^u/N_s$ and considering eq 7 we can write

$$w^u = \frac{N_s^u}{N_s^u + N_s^v} = \frac{1}{1 + N_s^v/N_s^u} = \frac{1}{1 + (1/K^x)N^v/N^u} \tag{8}$$

Since the fraction N^v/N^u can be expressed with f^u as $N^v/N^u = 1/f^u - 1$, we get

$$w^u = \frac{1}{1 + \frac{1}{K^x}\left(\frac{1}{f^u} - 1\right)} \tag{9}$$

If the partition coefficient is $K^x = 1$, it follows $w^u = f^u$ as expected. That is, if the spin probe does not show a preference for one of the phases, the fraction of the lipid phase and the proportion of the corresponding spectral component will be equal. Equation 9 also clearly shows that one of the three quantities w, f, and K^x can be determined if the other two are known.

It is more common to use a concentration partition coefficient, which is expressed with concentrations instead of mole fractions

$$K = \frac{c_s^u}{c_s^v} = \frac{N_s^u}{N_s^v}\frac{V^v}{V^u} = K^x\frac{V^v/N^v}{V^u/N^u} \tag{10}$$

where V^i is the volume of phase i, while the fraction V^i/N^i represents the average effective molecular volume in phase i. Combining eqs 8 and 10 we get

$$w^u = \frac{1}{1 + (1/K)V^v/V^u} \tag{11}$$

For volume V^i of phase i we will assume that it can be written as a linear combination of effective molecular volumes $V_{1,2}^0$ of lipids 1 and 2. We therefore obtain

$$\frac{V^v}{V^u} = \frac{N_1^v V_1^{v,0} + N_2^v V_2^{v,0}}{N_1^u V_1^{u,0} + N_2^u V_2^{u,0}} = \frac{N^v}{N^u}\frac{x_1^v V_1^{v,0} + x_2^v V_2^{v,0}}{x_1^u V_1^{u,0} + x_2^u V_2^{u,0}} = \left(\frac{1}{f^u} - 1\right)\frac{V_1^{v,0}}{V_1^{u,0}}\frac{1 + x_2^v(V_2^{v,0}/V_1^{v,0} - 1)}{1 + x_2^u(V_2^{u,0}/V_1^{u,0} - 1)} \tag{12}$$

If in the first approximation temperature dependence of K and temperature dependence of the ratios of effective molecular volumes are neglected, the expression for temperature dependence of the proportion of a spectral component corresponding to phase u can be derived from eqs 11 and 12:

$$w^u(T) = \frac{1}{1 + \frac{1}{K}\left(\frac{1}{f^u(T)} - 1\right)\frac{V_1^{v,0}}{V_1^{u,0}}\frac{1 + x_2^v(T)[V_2^{v,0}/V_1^{v,0} - 1]}{1 + x_2^u(T)[V_2^{u,0}/V_1^{u,0} - 1]}} \tag{13}$$

Introducing approximate numerical values for the ratios of effective molecular volumes from the literature, eq 13 can serve as a basis for comparison of the calculated values of the proportion of the spectral component and the corresponding experimental values, i.e., for determination of the partition coefficient.

RESULTS

EPR Spectra of Lipid Phase Coexistence Regions. The aim of this subsection is to show that the EPR spectra of spin labeled liposomes at temperature and composition exhibiting lipid phase separation actually reflect the coexistence of different lipid phases. It can be nicely seen from Figures 4−6 that we can qualitatively describe a spectrum from a two phase coexistence region as a superposition of spectra from corresponding single phase regions.

EPR Spectra Decomposition. Spectral parameters and proportions of spectral components corresponding to particular lipid phases can be determined by EPR spectra decomposition. Our spectra were decomposed into two spectral components because at the most two different lipid phases can coexist in our experimental system according to the phase diagrams (Figures 2 and 3). Moreover, spectra of liposomes exhibiting coexistence regions can be qualitatively composed of two spectra of single phase liposomes (Figures 4−6). An example of decomposition is shown in Figure 7.

On the other hand, also spectra of single phase regions are not a purely single spectral component (data not shown), though one component is always highly dominant. Thus, simplification will be made, i.e., single lipid phase spectra will be described by only one spectral component.

Temperature Dependence of Order Parameter as an Indicator of Phase Transitions. Order parameter is one of the most sensitive spectral parameters and describes motional anisotropy of the spin label. It is connected to the time-averaged angular fluctuation of the acyl chain segment where the spin label (in our case nitroxide radical) is attached to the spin probe molecule. The temperature dependence of the order parameter was extracted from the recorded EPR spectra by spectral simulations. It is expected that this dependence shows discontinuity at temperatures corresponding to the completion of phase separations $Ld+S \rightarrow Ld$ and $Ld+Lo \rightarrow Ld$, while S and Lo phases are much more ordered than the Ld phase.

In Figure 8 results of measurement of the order parameter of the spectral component exhibiting higher ordering for the mixture DMPC/DPPC with different amounts of DPPC are shown. The transition temperatures, above which the order parameter drops discontinuously and which depend on the amount of added DPPC (solid arrows in Figure 8), agree quite well with the temperatures of the main phase transition T_m or temperatures corresponding to the completion of phase separation $Ld+S \rightarrow Ld$ for a particular composition in the range from 297 K for pure DMPC[18] to 315 K for pure DPPC.[19] Figure 8 also points to the appearance of the so-

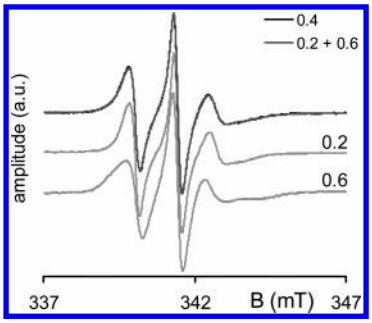

Figure 4. Comparison of experimental and calculated EPR spectrum. The experimental spectrum was obtained from spin labeled DMPC/DPPC liposomes with composition corresponding to the coexistence region of liquid-disordered phase and gel phase $Ld+S$ ($x_{DPPC}^0 = 0.4$, $T = 302$ K). The calculated spectrum is the superposition of the spectra of single lipid phase regions $x_{DPPC}^0 = 0.2$ (phase Ld) and $x_{DPPC}^0 = 0.6$ (phase S).

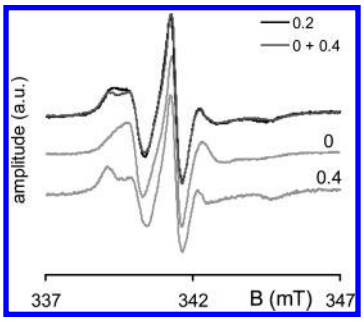

Figure 5. Comparison of experimental and calculated EPR spectrum. The experimental spectrum was obtained from spin labeled DMPC/Chol liposomes with composition corresponding to the coexistence region of gel phase and liquid-ordered phase $S+Lo$ ($x_{Chol}^0 = 0.2$, $T = 294$ K, $T < T_m$). The calculated spectrum is superposition of spectra of single lipid phase regions $x_{Chol}^0 = 0$ (phase S) and $x_{Chol}^0 = 0.4$ (phase Lo).

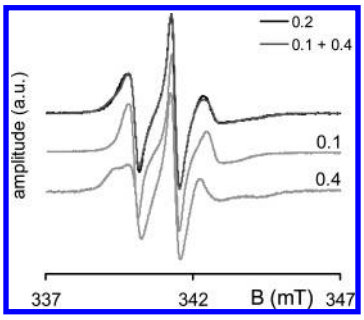

Figure 6. Comparison of experimental and calculated EPR spectrum. The experimental spectrum was obtained from spin labeled DMPC/Chol liposomes with composition corresponding to the coexistence region of liquid-disordered phase and liquid-ordered phase $Ld+Lo$ ($x_{Chol}^0 = 0.2$, $T = 306$ K, $T > T_m$). The calculated spectrum is superposition of spectra of single lipid phase regions $x_{Chol}^0 = 0.1$ (phase Ld) and $x_{Chol}^0 = 0.4$ (phase Lo).

called ripple phase[20] above the pretransition temperature T_p, which is 288 K for pure DMPC[18] (dashed arrow in Figure 8) and 308 K for pure DPPC.[19] It can be seen that for temperatures between T_p and transition temperatures for a particular composition the value of the order parameter decreases faster than for lower temperatures.

In Figure 9 temperature dependence of the order parameter of the spectral component exhibiting higher ordering is presented for the mixture DMPC/Chol with a different amount of cholesterol. Above T_m for pure DMPC (solid arrow in Figure 9) the order parameter drops discontinuously for

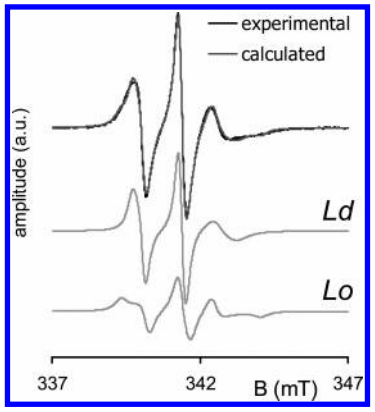

Figure 7. Experimental EPR spectrum of spin labeled DMPC/Chol liposomes ($x_{Chol}^0 = 0.2$, $T = 306$ K, $T > T_m$) compared with the calculated (fitted) spectrum. The fitted spectrum is decomposed into two spectral components corresponding to coexisting lipid phases, in this case phases Ld and Lo, respectively.

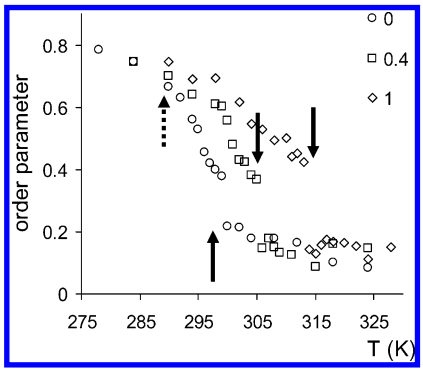

Figure 8. Temperature dependence of the order parameter of the spectral component exhibiting higher ordering for mixture DMPC/DPPC: $x_{DPPC}^0 = 0$, 0.4, 1. Solid arrows show T_m or temperature corresponding to the completion of phase separation $Ld+S \rightarrow Ld$ for a particular composition obtained from the phase diagram (Figure 2). A dashed arrow indicates pretransition temperature T_p for pure DMPC. The estimate of uncertainty in order parameter is ± 0.02.

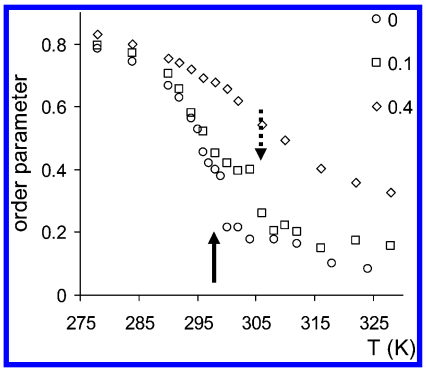

Figure 9. Temperature dependence of order parameter of a spectral component exhibiting higher ordering for the mixture DMPC/Chol: $x_{Chol}^0 = 0$, 0.1, 0.4. The solid arrow shows T_m for pure DMPC. The dashed arrow shows temperature T_{od} of the completion of phase separation $Ld+Lo \rightarrow Ld$ for $x_{Chol}^0 = 0.1$ obtained from the phase diagram (Figure 3). The estimate of uncertainty in the order parameter is ± 0.02.

$x_{Chol}^0 = 0$ as expected due to the phase transition $S \rightarrow Ld$. Similarly for $x_{Chol}^0 = 0.1$ the order parameter shows a discontinuous drop close to the temperature T_{od} corresponding to the completion of phase separation $Ld+Lo \rightarrow Ld$ (dashed arrow in Figure 9). Again it can be seen that in the temperature region between the pretransition temperature T_p

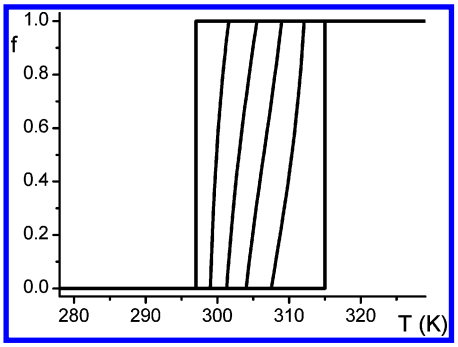

Figure 10. Temperature dependence of fractions $f^{Ld}(T)$ for the mixture DMPC/DPPC: $x_{DPPC}^0 = 0$, 0.2, 0.4, 0.6, 0.8, 1 (from left to right).

for pure DMPC and the temperature of the main phase transition T_m for pure DMPC the value of the order parameter decreases faster than in the region below T_p. This faster decrease is not present for $x_{Chol}^0 = 0.4$.

Calculation of Fraction of Lipid Phases and Proportion of Spectral Components. In accordance with the lever rule (eq 4) the temperature dependence of the fraction of the *Ld* phase can be calculated in the region of lipid phase coexistence *Ld*+*S* from the known phase diagram of the mixture DMPC/DPPC (Figure 2, Table 1)

$$f^{Ld}(T) = \frac{x_{DPPC}^{S}(T) - x_{DPPC}^{0}}{x_{DPPC}^{S}(T) - x_{DPPC}^{Ld}(T)} \tag{14}$$

where $x_{DPPC}^{Ld}(T)$ and $x_{DPPC}^{S}(T)$ are values of DPPC mole fractions at corresponding phase boundaries. Outside the coexistence region $f^{Ld}(T)$ is equal to 0 for lower temperatures and $f^{Ld}(T)$ is equal to 1 for higher temperatures. The temperature dependence of fraction $f^{Ld}(T)$ for different x_{DPPC}^0 is shown in Figure 10.

Similarly, we can extract information on the fraction of lipid phases from the known phase diagram of the mixture DMPC/Chol (Figure 3, Table 1). In Figure 3 it can be seen that at low concentrations of cholesterol and below the T_m fraction of the *S* phase $f^{S}(T)$ is equal to 1, while for the $T > T_m$ fraction of the *Ld* phase $f^{Ld}(T)$ is equal to 1. At high concentrations of the cholesterol fraction of the *Lo* phase $f^{Lo}(T)$ is 1; therefore, fractions $f^{S}(T)$ and $f^{Ld}(T)$ are 0. In accordance with the lever rule (eq 4) for temperatures $T < T_m$ and in the phase coexistence region *S*+*Lo* we can write

$$f^{S}(T) = \frac{x_{Chol}^{Lo}(T) - x_{Chol}^{0}}{x_{Chol}^{Lo}(T) - x_{Chol}^{S}(T)} \tag{15}$$

while for temperatures $T > T_m$ (coexistence region *Ld*+*Lo*) we have

$$f^{Ld}(T) = \frac{x_{Chol}^{Lo}(T) - x_{Chol}^{0}}{x_{Chol}^{Lo}(T) - x_{Chol}^{Ld}(T)} \tag{16}$$

where $x_{Chol}^{Lo}(T)$, $x_{Chol}^{S}(T)$, and $x_{Chol}^{Ld}(T)$ represent cholesterol molar fractions at corresponding phase boundaries. Because $x_{Chol}^{S}(T_m)$ is equal to $x_{Chol}^{Ld}(T_m)$ (see Figure 3) it follows from eqs 15 and 16 that $f^{S}(T_m)$ and $f^{Ld}(T_m)$ are the same. Therefore, above the T_m phase *S* "melts" into phase *Ld*. Consequently, diagrams of temperature dependence of fractions for different x_{Chol}^0 are shown in Figure 11: $f^{S}(T)$ is shown below T_m and $f^{Ld}(T)$ is shown above T_m.

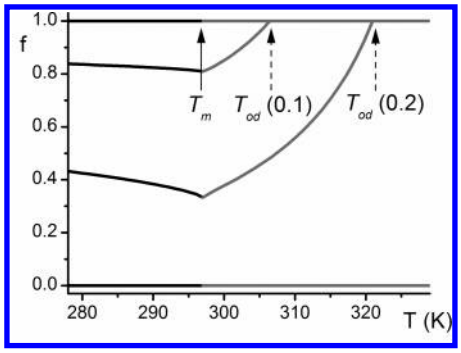

Figure 11. Temperature dependence of fractions f^{S} for $T < T_m$ (black lines) and f^{Ld} for $T > T_m$ (gray lines) for the mixture DMPC/Chol: $x_{Chol}^0 = 0$, 0.1, 0.2, 0.4 (from top to bottom). The solid arrow shows T_m for pure DMPC. The dashed arrows show temperature T_{od} of the completion of the phase separation *Ld*+*Lo* → *Ld* for $x_{Chol}^0 = 0.1$ and 0.2 obtained from the phase diagram (Figure 3).

The temperature dependence of the proportion of spectral components can be determined from the dependence of the fraction of the corresponding lipid phase taking into account the partition coefficient of the used spin probe between different lipid phases. For the DMPC/DPPC mixture we get from eq 13 and Table 1

$$w^{Ld}(T) = \frac{1}{1 + \frac{1}{K}\left(\frac{1}{f^{Ld}(T)} - 1\right)\frac{V_{DMPC}^{S,0}}{V_{DMPC}^{Ld,0}}\frac{1 + x_{DPPC}^{S}(T)[V_{DPPC}^{S,0}/V_{DMPC}^{S,0} - 1]}{1 + x_{DPPC}^{Ld}(T)[V_{DPPC}^{Ld,0}/V_{DMPC}^{Ld,0} - 1]}} \tag{17}$$

The estimates of values of ratios of effective molecular volumes were obtained from the literature (see Table 2). If these values and the values of DPPC mole fractions at corresponding phase boundaries are taken into account, eq 17 can be simplified to a first approximation into

$$w^{Ld}(T) \approx \frac{1}{1 + \frac{1}{K}\left(\frac{1}{f^{Ld}(T)} - 1\right)} \tag{18}$$

If *K* is close to 1, the proportion $w^{Ld}(T)$ will be approximately equal to $f^{Ld}(T)$.

In the same way the temperature dependence of the proportion of spectral components can be calculated for the mixture DMPC/Chol. In accordance with eq 13 we get for $T < T_m$

$$w^{S}(T) = \frac{1}{1 + \frac{1}{K}\left(\frac{1}{f^{S}(T)} - 1\right)\frac{V_{DMPC}^{Lo,0}}{V_{DMPC}^{S,0}}\frac{1 + x_{Chol}^{Lo}(T)[V_{Chol}^{Lo,0}/V_{DMPC}^{Lo,0} - 1]}{1 + x_{Chol}^{S}(T)[V_{Chol}^{S,0}/V_{DMPC}^{S,0} - 1]}} \tag{19}$$

and for $T > T_m$

$$w^{Ld}(T) = \frac{1}{1 + \frac{1}{K}\left(\frac{1}{f^{Ld}(T)} - 1\right)\frac{V_{DMPC}^{Lo,0}}{V_{DMPC}^{Ld,0}}\frac{1 + x_{Chol}^{Lo}(T)[V_{Chol}^{Lo,0}/V_{DMPC}^{Lo,0} - 1]}{1 + x_{Chol}^{Ld}(T)[V_{Chol}^{Ld,0}/V_{DMPC}^{Ld,0} - 1]}} \tag{20}$$

Table 2. Estimates of Ratios of Effective Molecular Volumes from Literature

mixture			
DMPC/DPPC[a]	$\frac{V_{DMPC}^{S,0}}{V_{DMPC}^{Ld,0}} \approx 0.95$	$\frac{V_{DPPC}^{S,0}}{V_{DMPC}^{S,0}} \approx 1.09$	$\frac{V_{DPPC}^{Ld,0}}{V_{DMPC}^{Ld,0}} \approx 1.10$
DMPC/Chol ($T < T_m$)[b]	$\frac{V_{DMPC}^{Lo,0}}{V_{DMPC}^{S,0}} \approx 1$	$\frac{V_{Chol}^{Lo,0}}{V_{DMPC}^{Lo,0}} \approx 0.56$	$\frac{V_{Chol}^{S,0}}{V_{DMPC}^{S,0}} \approx 0.56$
DMPC/Chol ($T > T_m$)[c]	$\frac{V_{DMPC}^{Lo,0}}{V_{DMPC}^{Ld,0}} \approx 0.95$	$\frac{V_{Chol}^{Lo,0}}{V_{DMPC}^{Lo,0}} \approx 0.56$	$\frac{V_{Chol}^{Ld,0}}{V_{DMPC}^{Ld,0}} \approx 0.53$

[a] Values were obtained from specific volume of DMPC and DPPC as well as the change of specific volume of DMPC and DPPC at the main phase transition.[21] [b] It was assumed that for the volume of the cholesterol molecule the value of the molecular volume in crystal[22] can be used because cholesterol is a relatively rigid molecule.[23] [c] The change of the volume of the DMPC molecule from the *Lo* to the *Ld* phase was estimated from data obtained by molecular dynamics simulations.[23,24]

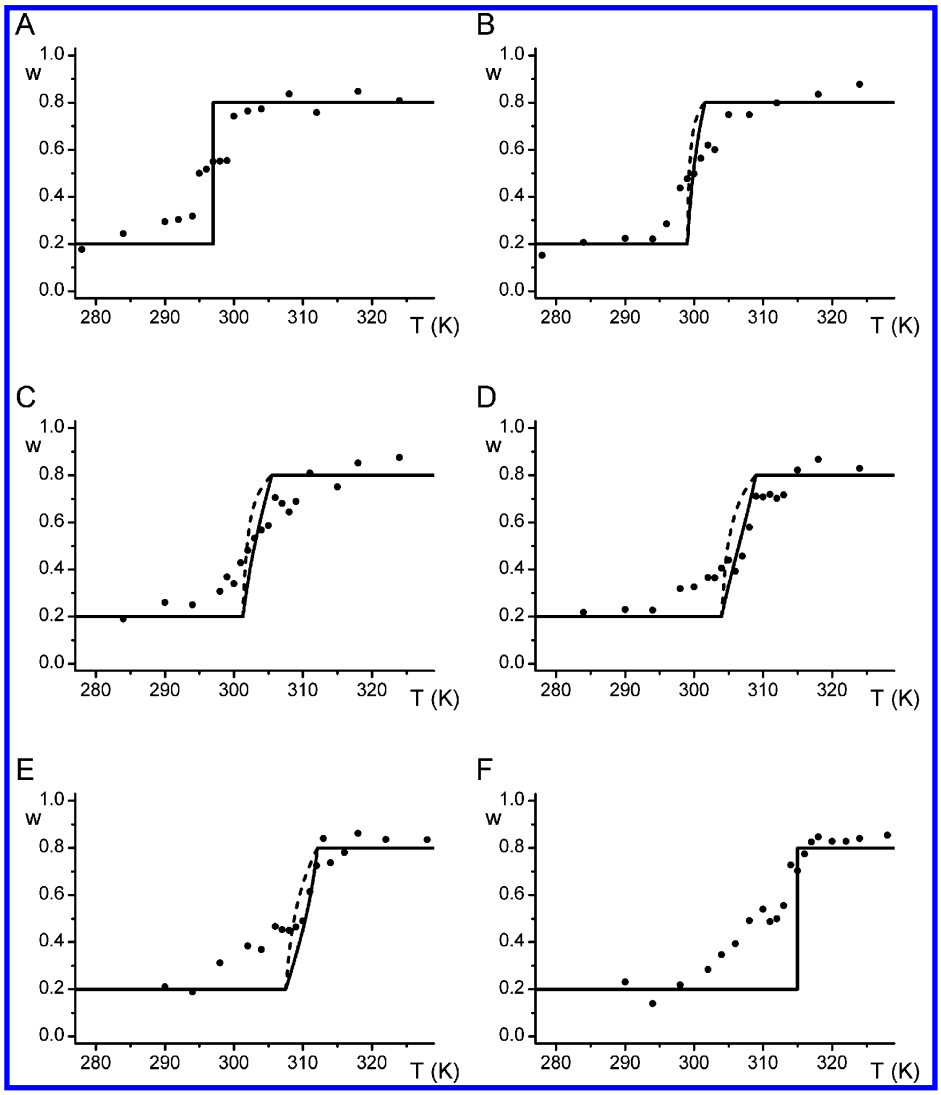

Figure 12. Temperature dependence of measured (points) and calculated (lines) proportions $w^{Ld}(T)$ for mixture DMPC/DPPC: (A) $x_{DPPC}^0 = 0$, (B) $x_{DPPC}^0 = 0.2$, (C) $x_{DPPC}^0 = 0.4$, (D) $x_{DPPC}^0 = 0.6$, (E) $x_{DPPC}^0 = 0.8$, and (F) $x_{DPPC}^0 = 1$. The solid lines show calculated values according to eq 18 for $K = 1$, and the dashed lines calculated values for $K = 4$. The estimate of uncertainty in measured values of the proportion is ± 0.05.

The values of ratios of effective molecular volumes used for calculations are listed in Table 2.

Comparison of Calculated and Experimental Values of Fraction of Lipid Phases and Proportion of Spectral Components. In Figure 12 experimentally determined values for proportions are compared to the calculated values of proportions for the mixture DMPC/DPPC. The solid lines in Figure 12 represent calculations according to eq 18 with K equal to 1. This value was chosen because it was established in different experiments, that the level of ordering

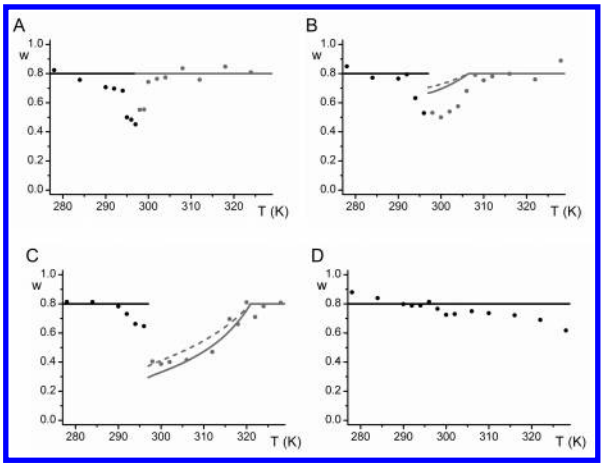

Figure 13. Temperature dependence of measured (points) and calculated (lines) proportions for the mixture DMPC/Chol: (A) $x_{Chol}^0 = 0$, (B) $x_{Chol}^0 = 0.1$, (C) $x_{Chol}^0 = 0.2$, and (D) $x_{Chol}^0 = 0.4$. The calculated values are shown as a sum of proportions w^S+w^{Lo} for $T < T_m$ (black lines), while for the $T > T_m$ proportion w^{Ld} is shown (solid gray lines show calculated values according to eq 20 for $K = 1$ and dashed gray lines calculated values for $K = 1.5$). The estimate of uncertainty in measured values of proportion is ± 0.05.

does not effect much partitioning of fatty acid spin and fluorescence probes or if it does, then it is more probable that they show a tendency toward less ordered phases.[4,7,25] So for comparison calculated values for K equal to 4 are also presented in Figure 12 (dashed lines).

In Figure 13 the comparison between experimentally determined and calculated values of proportions for mixture DMPC/Chol is shown. It can be seen that the order parameter does not change significantly at low temperatures for samples with a different content of cholesterol (Figure 9). Consequently, characterization of the EPR spectrum corresponding to the *S*+*Lo* coexistence region reveals an average picture of these two phases, meaning that we cannot distinguish well between these two phases by spectra decomposition. Consequently, we decided to show the calculated proportion as w^S+w^{Lo} instead of w^S for $T < T_m$. For the $T > T_m$ proportion $w^{Ld}(T)$ was calculated according to eq 20 with the value of the partition coefficient K set to 1 and the values for ratios of effective molecular volumes taken from Table 2.

For comparison the dependence of the calculated proportion for $x_{Chol}^0 = 0.1$, 0.2 is shown also for K equal to 1.5 in Figure 13 (see dashed lines in Figure 13B,C). This value of partition coefficient would mean that a spin probe shows a preference for the *Ld* phase. For $x_{Chol}^0 = 0.2$ (Figure 13C) the change is not significant, while for $x_{Chol}^0 = 0.1$ (Figure 13B), the agreement between measured and calculated values becomes worse.

DISCUSSION

The EPR spectra of spin labeled liposomes of binary lipid mixtures DMPC/DPPC or DMPC/Chol were decomposed into two spectral components, as we expect that at most two lipid phases will coexist at a particular temperature and composition (Figures 2 and 3). By the EPR spectra decomposition we were able to extract information about motional characteristics (e.g. order parameter) of the spin probe as well as the proportion of spectral components.

It was already mentioned that also spectra of single phase regions can be fitted by two spectral components. This points out that our spin label can detect also other motional patterns, which can originate either in a not so strongly fixed vertical position of the spin probe or in weak local interactions with neighboring lipid molecules. In general one would have to fit spectra with a few spectral components and map different motional patterns. This can be done by the GHOST condensation method,[26] but with this method determination of proportions is not so accurate. Consequently, when the expected number of spectral components is small, the best fit approach is more appropriate for quantitative analysis. Since the contribution of the second spectral component in spectra of single lipid phase liposomes is not so large (proportion around 0.2), single phase spectra were described by only one spectral component.

In the temperature dependence of the order parameter in the DMPC/DPPC mixture (Figure 8) the discontinuity occurs near the temperature of the main phase transition T_m or temperatures corresponding to the completion of phase separation $Ld+S \rightarrow Ld$ for a particular composition. A steeper decrease of the order parameter in the temperature interval between the temperature of pretransition and the temperature of the main phase transition $T_p < T < T_m$ might reflect the presence of the ripple phase, where the order parameter more quickly decreases with temperature.[27] In Figure 9 the temperature dependence of the order parameter for the DMPC/Chol mixture is shown. Temperatures at which discontinuities are present in the graphs agree reasonably well with the temperatures expected from the phase diagram (see arrows in Figure 9). Similar to the case of the DMPC/DPPC mixture at the molar fractions of cholesterol $x_{chol}^0 = 0$ and 0.1 the steeper slope of decrease of the order parameter for $T_p < T < T_m$ is present. This effect is not seen for $x_{chol}^0 = 0.4$, while with the increase of cholesterol concentration the ripple phase slowly fades away.[22,28] We can conclude that results for the ordering of lipids obtained from the EPR spectra decomposition gives us results that qualitatively agree with results that are expected from the shape of phase diagrams.

From temperature dependence of the proportion of the *Ld* phase for the DMPC/DPPC mixture (Figure 12) it can be seen that the temperature at which the *S* phase "melts" to the *Ld* phase coincides reasonably well with the temperature of the main phase transition. On the other hand, the width of the temperature interval in which the increase of w^{Ld} happens is much broader compared to the expected calculated width represented by calculated lines, disabling us to estimate the partition coefficient between *S* and *Ld* lipid phases. The increase of w^{Ld} below T_m might be a consequence of the presence of the ripple phase, while this phase contains some amount of disordered lipids.[29,30] If the partition coefficient is set to be higher than 1 (dashed lines in Figure 12), the discrepancy between measured and calculated values becomes higher. So qualitatively we might conclude that most likely our spin probe does not show a preference for one of the phases.

The difference between measured proportions and the sum of calculated proportions for gel and liquid-ordered phase w^S+w^{Lo} calculated below T_m (Figure 13) might be a consequence of the presence of the ripple phase. For $x_{Chol}^0 = 0.1$ in 0.2 (Figure 13B,C) the reason might also be that

the sum w^S+w^{Lo} no longer represents the measured points, while opposite to low temperatures spectra of *S* and *Lo* phase can be distinguished, so measured points represent w^{Lo} when temperature approaches T_m. Measured proportions qualitatively agree with the calculated ones in the temperature interval $T > T_m$. (Figure 13). Temperatures at which proportion w^{Ld} increases to the maximum value for molar fractions of cholesterol $x_{Chol}{}^0 = 0.1$ in 0.2 agree well with temperatures T_{od} corresponding to the completion of phase separation $Ld+Lo \rightarrow Ld$ as deduced from the phase diagram (Figure 3). In addition, the proportion of the spectral component corresponding to the *Lo* phase for $x_{Chol}{}^0 = 0.4$ (Figure 13D) shows only a small change with temperature. This is in agreement with the expectation that this proportion will be constant with temperature, while for $x_{Chol}{}^0 = 0.4$ only the *Lo* phase is present for the observed temperature interval (Figure 3). From the quantitative point of view it can be seen that in the case of $x_{Chol}{}^0 = 0.1$ there is a significant difference between measured and calculated values for proportions in the temperature interval $T_m < T < T_{od}$ (see Figure 13B). This difference could be a consequence of an unsuitable choice of partition coeficient $K = 1$ for calculating proportion w^{Ld} in accordance with eq 20. For this reason also the calculated proportion is shown if the partition coefficient was put to $K = 1.5$ (dashed line in Figure 13B). It turns out that the difference between measured and calculated values is even larger in this case. To lower the difference we would have to put $K < 1$. But such a value (indicating a preference of spin probe for more ordered lipid regions) is not expected for fatty acid spin probes.[7,31] It seems at least qualitatively that our spin probe does not show preference for the *Lo* or *Ld* phase.

At the end we have to depict the problem of the use of phase boundaries in the calculation of fractions of lipids in particular lipid phases in accordance with eqs 14−16. Namely, phase boundaries are determined from phase diagrams (Figures 2 and 3), which are not univocal as their shape can depend on the experimental method applied to determine it. Then as already mentioned, the ripple phase was not taken into account in the presented phase diagrams. In addition, different experiments show that also other phases can be present in phase diagrams.[32,33] Thus, one has to be aware that calculated proportions are largely dependent on the calculation of lipid fractions from a phase diagram and by that on the shape of phase diagram.

As we have already mentioned we could not accurately determine a partition coefficient for our spin probe between the *S* and *Ld* lipid phases. Likewise, it was not possible to ascertain a partition coefficient between the *S* and *Lo* phases, while at low temperatures we could not clearly distinguish between the EPR spectra of the *S* and *Lo* phases. On the other hand, we expect that the gel phase has a lower relevance for biological membranes at physiological temperatures. In this view determination of the partition coefficient of the spin probe between liquid-disordered phase *Ld* and liquid-ordered phase *Lo* is more important, while there are indications that lipid domains resembling the *Lo* phase exist in biological membranes (Ge et al. 1999, Brown and London 2000, Schütz et al. 2000). Because of high uncertainty of the proportions (see Figure 13) we can only approximately estimate that the partition coefficient between *Ld* and *Lo* is close to 1. Therefore, measured proportions of spectral components from the procedure of the EPR spectra decomposition for MeFASL(10,3) are to a first approximation equal to fractions of corresponding lipid domain types in biological membranes.

ACKNOWLEDGMENT

This work was carried out with the financial support of the Ministry of Education, Science and Sport of the Republic of Slovenia.

REFERENCES AND NOTES

(1) Shimshick, E. J.; McConnell, H. M. Lateral Phase Separation in Phospholipid Membranes. *Biochemistry* **1973**, *12*, 2351−2360.
(2) Bloom, M.; Thewalt, J. L. Time and distance scales of membrane domain organization. *Mol. Membr. Biol.* **1995**, *12*, 9−13.
(3) Arsov, Z.; Schara, M.; Štrancar, J. Quantifying the Lateral Lipid Domain Properties in Erythrocyte Ghost Membranes Using EPR−Spectra Decomposition. *J. Magn. Reson.* **2002**, *157*, 52−60.
(4) Mesquita, R. M. R. S.; Melo, E.; Thompson, T. E.; Vaz, W. L. C. Partitioning of Amphiphiles between Coexisting Ordered and Disordered Phases in Two-Phase Lipid Bilayer Membranes. *Biophys. J.* **2000**, *78*, 3019−3025.
(5) Arsov, Z.; Schara, M.; Zorko, M.; Štrancar, J. The membrane lateral domain approach in the studies of lipid−protein interaction of GPI-anchored bovine erythrocyte acetylcholinesterase. *Eur. Biophys. J.* **2004**, *33*, 715−725.
(6) Mabrey, S.; Sturtevant, J. M. Investigation of phase transitions of lipids and lipid mixtures by high sensitivity differential scanning calorimetry. *Proc. Natl. Acad. Sci. U.S.A.* **1976**, *73*, 3862−3866.
(7) Almeida, P. F. F.; Vaz, W. L. C.; Thompson, T. E. Lateral Diffusion in the Liquid Phases of Dimyristoylphosphatidylcholine/Cholesterol Lipid Bilayers: A Free Volume Analysis. *Biochemistry* **1992**, *31*, 6739−6747.
(8) Ge, M.; Field, K. A.; Aneja, R.; Holowka, D.; Baird, B.; Freed, J. H. Electron spin resonance characterization of liquid ordered phase of detergent-resistant membranes from RBL-2H3 cells. *Biophys. J.* **1999**, *77*, 925−933.
(9) Brown, D. A.; London, E. Structure and Function of Sphingolipid- and Cholesterol-rich Membrane Rafts. *J. Biol. Chem.* **2000**, *275*, 17221−17224.
(10) Schütz, G. J.; Kada, G.; Pastushenko, V. P.; Schindler, H. Properties of lipid microdomains in a muscle cell membrane visualized by single molecule microscopy. *EMBO J.* **2000**, *19*, 892−901.
(11) Budil, D. E.; Lee, S.; Saxena, S.; Freed, J. H. Nonlinear-Least-Squares Analysis of Slow-Motion EPR Spectra in One and Two Dimensions Using a Modified Levenberg−Marquardt Algorithm. *J. Magn. Reson. A* **1996**, *120*, 155−189.
(12) Tu, K.; Tobias, D. J.; Blasie, J. K.; Klein, M. L. Molecular Dynamics Investigation of the Structure of a Fully Hydrated Gel-Phase Dipalmitoylphosphatidylcholine Bilayer. *Biophys. J.* **1996**, *70*, 595−608.
(13) Venable, R. M.; Brooks, B. R.; Pastor, R. W. Molecular dynamics simulations of gel ($L_{\beta I}$) phase lipid bilayers in constant pressure and constant surface area ensembles. *J. Chem. Phys.* **2000**, *112*, 4822−4832.
(14) Štrancar, J.; Šentjurc, M.; Schara, M. Fast and accurate characterization of biological membranes by EPR spectral simulations of nitroxides. *J. Magn. Reson.* **2000**, *142*, 254−265.
(15) Štrancar, J. EPRSIM Version 5.7. Janez Štrancar, 1996−2005, http://www.ijs.si/ijs/dept/EPR/.
(16) Filipič, B.; Štrancar, J. Tuning EPR spectral parameters with a genetic algorithm. *Appl. Soft Comput.* **2001**, *1*, 83−90.
(17) Filipič, B.; Štrancar, J. Evolutionary Computational Support for the Characterization of Biological Systems. In *Evolutionary Computation in Bioinformatics*; Fogel, G. B., Corne, D. W., Eds.; Morgan Kaufmann Publishers: San Francisco, 2002; pp 279−294.
(18) Holopainen, J. M.; Lemmich, J.; Richter, F.; Mouritsen, O. G.; Rapp, G.; Kinnunen, P. K. J. Dimyristoylphosphatidylcholine/C16:0-Ceramide Binary Liposomes Studied by Differential Scanning Calorimetry and Wide- and Small-Angle X-Ray Scattering. *Biophys. J.* **2000**, *78*, 2459−2469.
(19) Heimburg, T. Mechanical aspects of membrane thermodynamics. Estimation of the mechanical properties of lipid membranes close to the chain melting transition from calorimetry. *Biochim. Biophys. Acta* **1998**, *1415*, 147−162.
(20) Copeland, B. R.; McConnell, H. M. The rippled structure in bilayer membranes of phosphatidylcholine and binary mixtures of phosphatidylcholine and cholesterol. *Biochim. Biophys. Acta* **1980**, *599*, 95−109.

(21) Nagle, J. F.; Wilkinson, D. A. Lecithin bilayers. Density measurements and molecular interactions. *Biophys. J.* **1978**, *23*, 159−175.
(22) Shieh, H.-S.; Hoard, L. G.; Nordman, C. E. The Structure of Cholesterol, *Acta Crystallogr.* **1981**, *B37*, 1538−1543.
(23) Smondyrev, A. M.; Berkowitz, M. L. Molecular Dynamics Simulation of the Structure of Dimyristoylphosphatidylcholine Bilayers with Cholesterol, Ergosterol, and Lanosterol. *Biophys. J.* **2001**, *80*, 1649−1658.
(24) Smondyrev, A. M.; Berkowitz, M. L. Structure of Dipalmitoylphosphatidylcholine/ Cholesterol Bilayer at Low and High Cholesterol Concentrations: Molecular Dynamics Simulation. *Biophys. J.* **1999**, *77*, 2075−2089.
(25) Tsuchida, K.; Tomizawa, K.; Hatta, I. Partitioning of Stearic Acid Spin Labels into Phospholipid Bilayers with Different Fluidities. *J. Phys. Soc. Jpn.* **1994**, *63*, 3894−3898.
(26) Štrancar, J.; Koklič, T.; Arsov, Z.; Filipič, B.; Stopar, D.; Hemminga, M. A. Spin Label EPR−Based Characterization of Biosystem Complexity. *J. Chem. Inf. Model.* **2005**, *45*, 394−406.
(27) Heimburg, T.; Würz, U.; Marsh, D. Binary phase diagram of hydrated dimyristoylglycerol-dimyristoylphosphatidylcholine mixtures. *Biophys. J.* **1992**, *63*, 1369−1378.
(28) Mortensen, K.; Pfeiffer, W.; Sackmann, E.; Knoll, W. Structural properties of a phosphatidylcholine-cholesterol system as studied by small-angle neutron scattering: ripple structure and phase diagram. *Biochim. Biophys. Acta* **1988**, *945*, 221−245.
(29) Tsuchida, K.; Hatta, I. ESR studies on the ripple phase in multilamellar phospholipid bilayers. *Biochim. Biophys. Acta* **1988**, *945*, 73−80.
(30) Heimburg, T. A Model for the Lipid Pretransition: Coupling of Ripple Formation with the Chain-Melting Transition. *Biophys. J.* **2000**, *78*, 1154−1165.
(31) Pokorny, A.; Almeida, P. F. F.; Melo, E. C. C.; Vaz, W. L. C. Kinetics of Amphiphile Association with Two-Phase Lipid Bilayer Vesicles. *Biophys. J.* **2000**, *18*, 267−280.
(32) McMullen, T. P. W.; McElhaney, R. N. New aspects of the interaction of cholesterol with dipalmitoylphosphatidylcholine bilayers as revealed by high-sensitivity differential scanning calorimetry. *Biochim. Biophys. Acta* **1995**, *1234*, 90−98.
(33) Karmakar, S.; Raghunathan, V. A. Cholesterol-Induced Modulated Phase in Phospholipid Membranes. *Phys. Rev. Lett.* **2003**, *91*, 098102.

CI0501793